university of groningen

faculty of science and engineering

INDUSTRIAL ENGINEERING & MANAGEMENT

Simulation of the energy flow of an offshore energy storage system

January 2020

Author: Thimo van Kessel
Student number: s2793091

First supervisor: A. Vakis
Second Supervisor: A.A. Geertsema

Abstract

Over the last decades, many new renewable energy sources have been developed. The fluctuations of wind and solar resources have posed a great challenge to produce a reliable supply of power. In order for renewable energy to completely replace fossil energy, a stable supply is required. Intermediate energy storage can help to reduce fluctuations in power generation by these renewable sources. The Ocean Battery, developed by the Ocean Grazer BV, offers a possibility to store renewable energy at the bottom of the ocean. To store potential energy, the system pumps fresh water into flexible bladders that are deflated by the pressure of the water column above. Like in any other storage system energy is lost in the process. This research delivers more insight in these losses and shows the round trip energy efficiency of the Ocean Battery.

Contents

1 Introduction

Over the last decades, many new renewable energy sources have been developed. These energy sources produce electricity from wind, solar and hydro power. In order for renewable energy sources to completely replace fossil energy, a stable supply is required (Sardianou & Genoudim, 2013). Since the weather is an unstable factor, the supply from these power sources is fluctuating and not as stable as fossil energy sources. The fluctuations of wind and solar resources have posed a great challenge to produce a reliable supply of power. Intermediate energy storage can help to reduce fluctuations in power generation by these renewable sources. For this purpose, the oversupply from renewable sources is stored in storage devices. According to Lee and Gushee (2008) massive electricity storage is the critical technology needed for the renewable power if it is to become a major source of energy. Furthermore, they indicate that energy storage system costs constitute about 30% of the total renewable power supply system costs.

During power shortage hours, these storage devices operate to serve the electric load. Batteries are the well- known solution for electric energy storage (Awan et al, 2019). When the supply from renewable sources is high, the energy is stored. This stored energy is used when the energy supply from the renewable source is low, resulting in a more stable supply. Moreover, energy storage is also used to supply electricity to the intraday power trading market.

In order to create a more stable supply, the Ocean Grazer group is developing an offshore energy storage system: the Ocean Battery. This system is located at the ocean floor and is used to store potential energy with the pressure of the ocean. The latest design of the energy storage system is shown in figure 1. In order to further develop this technology, more insight is needed in the energy flow of the storage system.

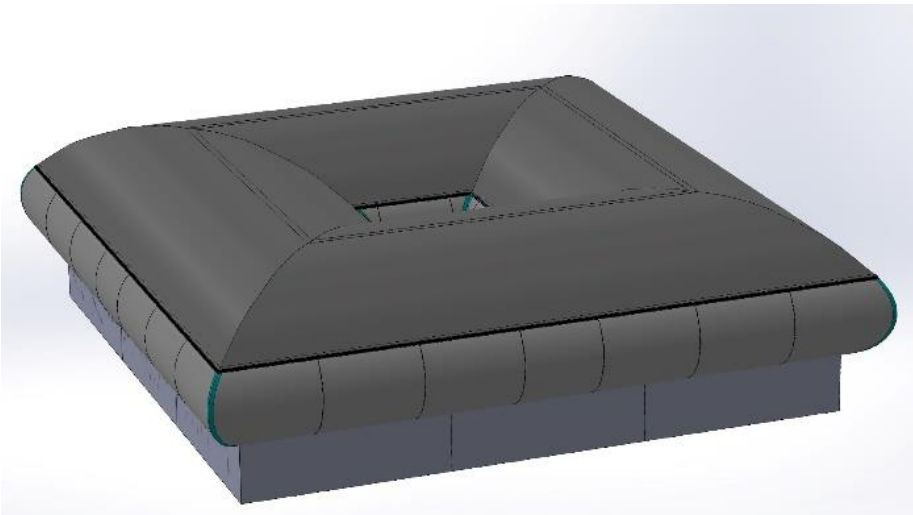

Figure 1: The design of the energy storage system created by the Ocean Grazer BV. The system is located on the ocean floor and it's measurements are 70 x 70 meter.

2 Problem analysis

Currently the round trip energy flow in the energy storage system is a black box. There are no specific numbers available for the energy losses in the different elements of the system. Therefore, it is not possible to make an accurate estimation about the overall efficiency of the energy storage. In order to get insight in the energy flow, more information is required about the subsystems that are involved. With the help of this information, it is possible to model and simulate the energy flow. A simulation will improve the changeability of the elements and parameters of the model. This will allow the Ocean Grazer BV to test different settings and measure the influence on the energy flow.

3 Stakeholder analysis

The stakeholders are the people, groups and organizations that show interest in the deliverables of this research. The stakeholders and their stake in this research are listed below:

- Marijn van Rooij, MSc, the CTO of the Ocean Grazer group, is the problem owner of this project. It is his responsibility to pursue new technological opportunities for the Ocean Grazer project. He is creating business cases from the knowledge that is gathered in academic studies. Currently, his focus is on further developing the energy storage system and therefore he is interested in the efficiency of the system.
- Prof. Dr. Antonis Vakis is a stakeholder in this research. He is the academic supervisor of this research and is mainly focusing on the scientific aspects. His focus will be on the physics used in this research and the model that is used to simulate the energy flow in the system.
- Drs. Wout Prins is the project manager and inventor of the Ocean Grazer and therefore a stakeholder in this project. His interest is mostly in the development of the technology used in the energy storage system. On the long-term he is interested in producing and selling the storage systems as a subsystem and in order to generate new financing for the development of the Ocean Grazer.

During the interview with the stakeholders multiple requirements are mentioned. The stakeholder requirements that are taken in consideration are described in the section below.

Since the design is still in the conceptual phase, all parameters in the model should be adaptive. The added value of a simulation can be found in the ease with which settings can be changed and tested. It is therefore important that this system is flexible and not only connected to one design. The systems energy supply should also be changeable, in order to provide testing possibilities with the Ocean Grazer instead of an electric pump.

The inputs of the simulation should be easy to enter in order to provide clear structure in the data and decrease the chance of errors. The output should be structured and accessible to read. This will facilitate easy comparison of test results.

4 System description

The function of the system is to store energy that is generated with the use of renewable energy sources. With the use of a flexible rubber bladder this energy can be stored at the ocean floor. As is described in the stakeholder analysis, the system is still in a conceptual phase, and the final application is not determined at this point in time. Two possible applications of the storage system are:

- To store and provide energy for the 15 minute intraday market.
- To facilitate a steady energy supply from renewable energy sources using peak shaving. Peak shaving is method that stores energy during peak generation and uses this to compensate during drops in energy supply.

A schematic overview of the system is shown in figure 2. The upper half of the figure shows the flow of the water during the charging and discharging phase. The lower half of the figure shows the energy flow of the system through the different elements. During the charging phase, a pump is used to pump fresh water from the reservoir to a rubber bladder. The fresh water is transported using a piping system and the bladder will keep the water from mixing with the salt water of the ocean. When the water is pumped in the bladder, the reservoir will be filled with fresh air. This fresh air enters through a long vertical tube that is connected to a floating device at sea level. The difference between the pressure of the ocean on the bladder and the atmospheric pressure in the reservoir results in potential energy.

In order to start the generation of electricity when the system is charged, a valve opens and water from the bladder flows through the piping system to the reservoir. In the middle of the piping system, the water flows through a turbine that is connected to a generator. With the use of this turbine driven generator, the potential energy that is stored in the bladder is converted in electricity.

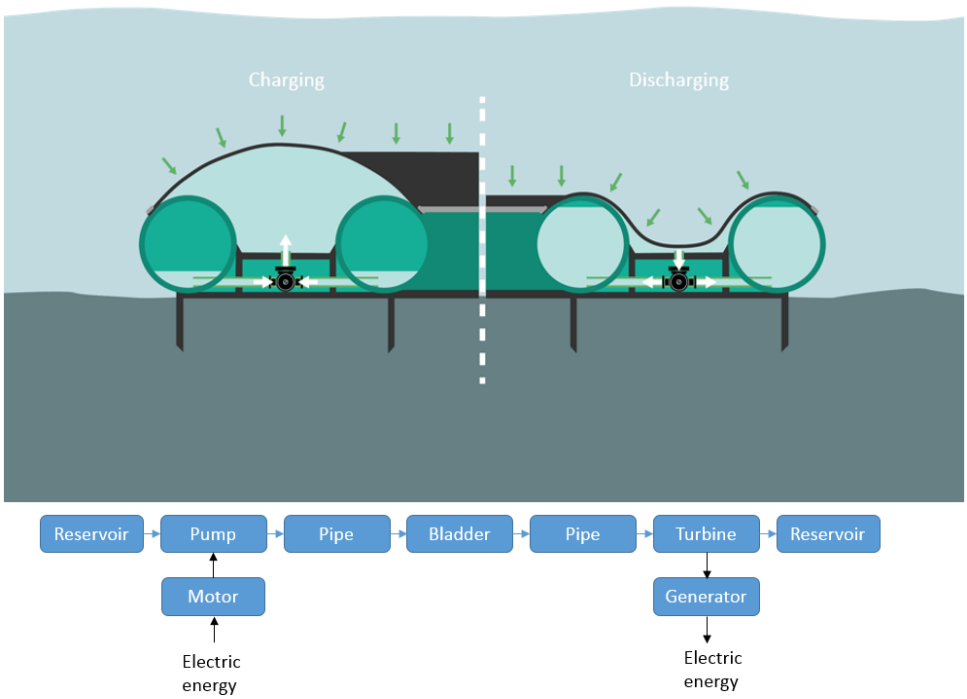

Figure 2: Overview of the Ocean Battery system. On top, the water flows through the system during charging and discharging phase. On the bottom, the block diagram shows the energy flow in the system.

In the scope of this research the focus is on the energy flow through the following six subsystems, also shown in figure 3:

- Electric motor
- Pump
- Piping system
- Bladder
- Turbine
- Generator

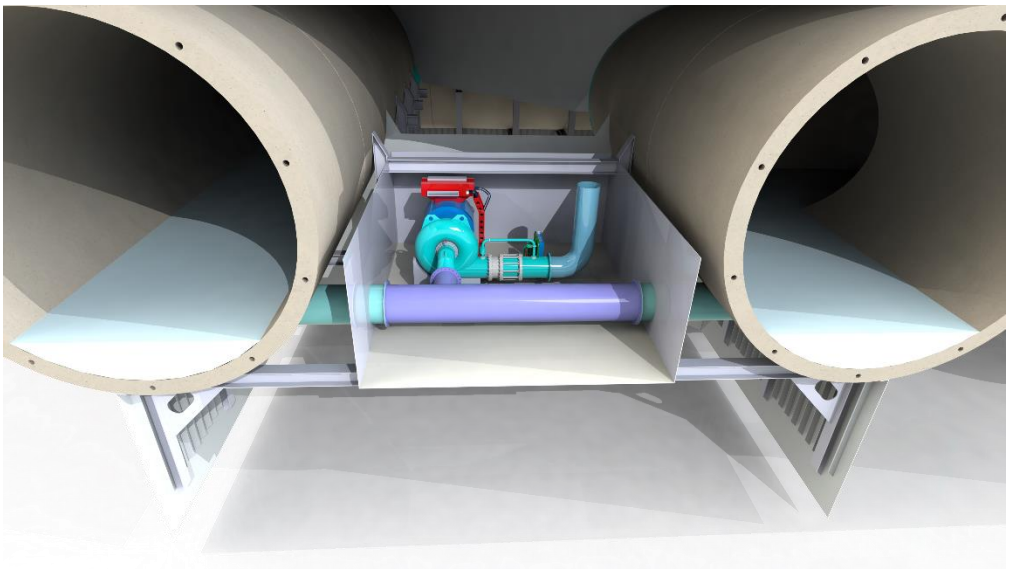

Figure 3: This figure shows a side view of the machine room in the Ocean Battery. The machine room includes an Electric motor, pump, pipe structure. In this design the pump is also used as the turbine and the motor is used as generator.

In order to get the round-trip energy efficiency of the system, calculations that describe the energy loss in the subsystems are required for all subsystems presented in figure 3.

To get more insight in the influence each of the subsystems has on the energy flow, it is necessary to develop a model of the system. Afterwards, a computer simulation of this model is created. In this simulation the different elements need to be replaceable and it should support changeable parameters. The simulation will provide the possibility to test different parameter settings, such as:

- System size
- Depth
- Storage capacity
- Charging and discharging speed
- Pipe size and length
- Different motor, pump, turbine and generator types
- Valve size

5 Problem definition

Currently there is a lack of information about the energy flow in the storage system. This information is necessary in order to create a model of the system. As a result it is not possible to simulate and test the behaviour of the elements in the system and there

influence on the energy flow. Therefore, the following problem statement is formulated for this research:

'The Ocean Grazer group has no insight in the energy efficiency of the energy storage system.'

6 Goal statement

The following research goal is formulated for this research:

'Deliver insight into the energy efficiency of the energy storage system of the Ocean Grazer group under changeable circumstances and settings.'

7 Research Questions

In order to reach the goal of this research, the following research question is defined:

'What is the round-trip efficiency of the energy storage system under changeable circumstances and settings?'

In order to answer the main research question, the following sub questions need to be answered:

'What information is needed about the elements to model the energy flow?'

'How can a simulation model of the energy flow be developed?'

'How can the simulation of the system be validated?'

8 Tools

The modelling of the elements is done using different formula's that describe the behaviour of the elements. These formulas are found in literature and in research articles. The energy flow in the system is based on the interaction of the elements and is shown by combining the elements in a model. It is the goal to create a simulation of this model. Using a simulation improves the changeability of separate elements and parameters, as is required by the stakeholders. This simulation is done with MATLAB, a software program created by MathWorks. The reason for this choice is based on the wide application of MATLAB in the Ocean Grazer group. By using MATLAB, earlier created models of the system can be analysed and partly applied in this research, where applicable.

9 Deliverable and Validation

The final deliverable of this research is a simulation of the energy storage system. This simulation generates the round-trip efficiency of the system under different circumstances and with different settings. The simulation will give more insight in the energy flow in the system and the elements can also be tested separately. The inputs of the system are the parameters as are discussed in the system description. The final output of the system is the round-trip energy efficiency of the energy storage system.

In the ideal situation, the delivered simulation will be tested on an experimental setup of the system. The results of the simulation are compared with the experimental setup that uses the same parameters. When the results from the experiments match with the results from the simulation model, the simulation is validated. However, in the current situation there is no experimental setup available apart from a small scale model that

can show the behaviour of the rubber bladder. Therefore, another method is used to validate the deliverable.

In order to validate the simulation, analytical calculations are performed. In these calculations the flowrates for both systems are calculated and checked with the values that resulted from the simulations. The error between the simulation results and the analytical will tell accuracy of the simulation. If this error is small enough, the simulation results are assumed to be accurate.

10 Risk analysis

During this research multiple assumptions are made based on the literature and previous research articles. A risk for this research is found in the fact that some of the information found in previous research can possibly contain mistakes. By using wrong information, the fundament for the conclusions of this research can possibly lose certainty. Therefore, it is extra important to clearly substantiate the assumptions that are made using only checked information that is confirmed in multiple sources.

11 Dynamical model of the energy flow in the Ocean Battery

In this chapter the energy flow is discussed in more detail. The flow of energy in the system can be separated in two phases: the charging phase and the discharging phase. In the charging phase, the water is pumped from the reservoir into the bladder where electric energy is stored as potential energy. In the discharging phase, the water flows form the bladder to the reservoir and the potential energy is converted back in electric energy. In order to create a simulation, the model is split in two separate models: the pump model and the turbine model.

In order to create a dynamical model of the energy storage, more information about the energy flows is necessary. Therefore it is now explained how the flowrate of the pump and turbine model can be calculated.

11.1 Flow rate pump model

In the pump model the charging stage of the Ocean battery is simulated. This model calculates the flow rate of the pump (Q_P) as a function of the electric power input (P_m). The pump model consists of two mechanical devices, an electro motor and a pump. The first device, the electro motor, converts electricity into mechanical energy. This mechanical energy is transferred to the pump using a shaft. The shaft drives the pump where the mechanical energy is transferred in kinetic energy that results in the flow of water. The efficiency of the motor (η_m) is a function of P_m (Eq. 2), and represents the amount of electric energy is transferred in mechanical energy by the electro motor. The efficiency of a motor is shown in the efficiency-power curve of the specific motor that is used.

The mechanical input power of the pump (P_P) is calculated with Eq. 1.

$$P_P = P_m \, \eta_m \tag{1}$$

$$\eta_m = f(P_m) \tag{2}$$

The pumping flowrate is used to calculate the amount of water that is transported from the reservoir to the bladder per unit of time. The pumping flowrate (Eq. 3) is a function of the total head of the pump and the pump efficiency (η_P) (Mousavi et al., 2019). The efficiency is a function of the flow rate of the pump, as is shown in

equation 4. The efficiency curve that shows the relation between the flowrate and the efficiency is provided by the pump manufacturer, or can be found during tests. An example of this curve for different pump types is shown in figure 4.

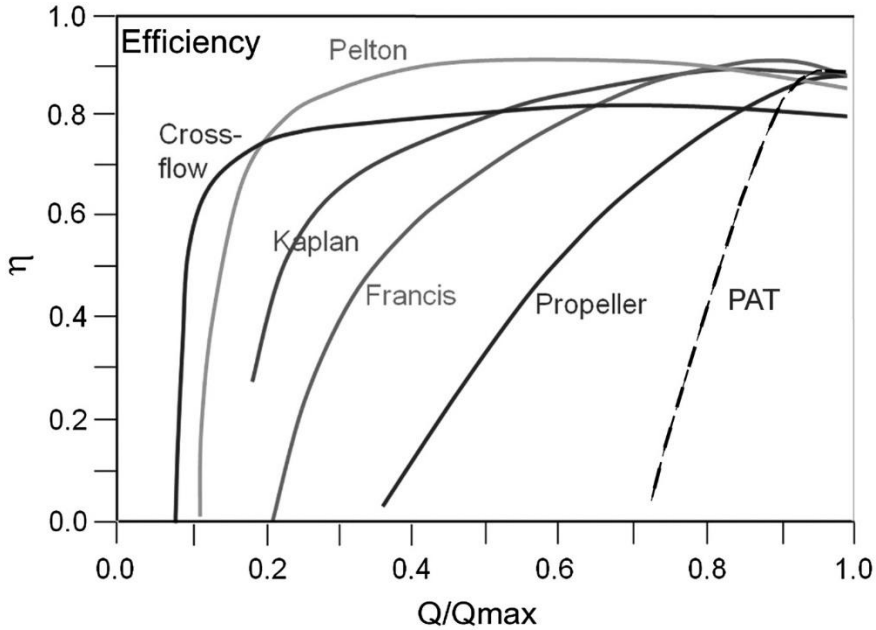

Figure 4: Flow rate – efficiency curve of a pump (Tidal barrage, 2015)

$$Q_P = \frac{P_P * \eta_P}{\rho * g * H_P} \tag{3}$$

where:

ρ is the density of the fluid $[kg/m^3]$
g is the standard acceleration due to gravity $[m/s^2]$
H_P is the total head of the pump $[m]$

$$\eta_P = f(Q_P) \tag{4}$$

The total head of the pump (H_p) is formed by the static head (H_s) and the head loss (H_{pl}) during the pump phase (Eq. 5). The static head is the result of the vertical difference between the water level in the reservoir and the sea water level. The H_s varies during the pumping stage since the water level in the reservoir decreases, while the sea water level remains the same. This decrease of the water level in the reservoir results in an increase in the H_s. The head loss is caused by the fiction between the water and the surface of the wall and fittings of the pipes. Since the head loss is a function of the flowrate, it varies during the pumping stage. The variable flowrate is the result of the change in the static head between the water level of the reservoir and the sea water level. The increase of the static head during the pumping stage results in a decrease of the flowrate (Eq. 3). This results in a change in the head loss due to friction.

Head losses due to friction are categorized as major losses and minor losses, that are discussed in the next chapter. H_{pl} is therefore expressed as the sum of major and minor losses (Eq. 6).

$$H_p = H_s + H_{pl} \tag{5}$$

$$H_{pl} = H_{major} + H_{minor} \tag{6}$$

The total head loss is calculated using the Darcy-Weisbach equation (Eq. 7) (Engineering Division Crane, 1969). In order to let the head loss be a function of the flowrate, all head losses are expressed in a K value.

$$H_{pl} = K\frac{v^2}{2g} \tag{7}$$

where:
v is the velocity of the fluid $[m/s^2]$
K is the loss coefficient $[-]$

11.2 Major head losses

The major head losses are caused by friction between the liquid and the inner surface of the pipes. The value K_{pipe} expresses the losses that result from this friction (Eq.8)

$$K_{pipe} = \frac{f_D L_p}{D_p} \tag{8}$$

where:
f_D is the Darcy-Weisbach friction factor $[-]$
L_p is the length of the pipe $[m]$
D_p is the diameter of the pipe $[m]$

The velocity (v) (Eq. 9) that is used to calculate the head loss in the pipe is derived from the flow rate (Eq. 3).

$$v = \frac{Q}{A} = \frac{Q_p}{0.25\pi {D_p}^2} \tag{9}$$

The Darcy-Weisbach friction factor (f_D) is a function of the Reynolds number and the relative roughness. The Reynolds number is function of the velocity (Eq.9), and is shown in equation 10. The relative roughness is the ratio of the pipe surface roughness (ε) to its diameter (D), or $\frac{\varepsilon}{D}$. There are different equation available to derive the friction factor, the selection of which is based on the Reynolds number.

In order to select the right method to calculate the friction factor, theory about flows in pipes is required. Flows in pipes are divided two flow types: Laminar flows and Turbulent flows. The flow type is selected with the use of Reynolds number.

$$\mathrm{Re} = \frac{\mathrm{vD}\rho}{\mu} \tag{10}$$

where:
μ is the viscosity of the fluid $[kg/ms]$

- Laminar flow: Re ≤ 2000
- Critical flow: 2000 < Re ≤ 4000

- Turbulent flow: Re > 4000

11.2.1 Laminar flows

In the case of laminar flow (Re<2000) the pipe roughness is not considered and the friction factor f_D (Eq. 11) is derived from the Hagen-Poiseuille equation (Chen, 1979):

$$f_D = \frac{64}{Re} \tag{11}$$

11.2.2 Critical flow

The region known as the critical flow occurs between Reynolds number of approximately 2000 and 4000. In this flow region, the flow can be either laminar or turbulent, depending upon several factors. These factors include changes in section, direction and obstruction in the flow.

11.2.3 Turbulent flows

When the flow is larger than critical, the flow is turbulent (Re>4000). A turbulent flow is characterised by random motion of fluid particles that flow in the opposite direction of the main flow. When calculations are done on a turbulent flow, the Haaland equation is used (Bansal, 2004). This method uses the absolute roughness and the pipe diameter combined with Reynolds number to find the Darcy-Weisbach friction factor. The Haaland equation is expressed in equation 12:

$$\frac{1}{\sqrt{f_D}} = 1.8log_{10}\left[\frac{6.9}{Re} + \left(\frac{\frac{\varepsilon}{D}}{3.7}\right)^{1.11}\right] \tag{12}$$

When we rewrite Eq. 12, we get the following equation that is used to determine the Darcy-Weisbach friction factor:

$$f_D = \left[1.8log_{10}\left(\frac{6.9}{Re} + \left(\frac{\frac{\varepsilon}{D}}{3.7}\right)^{1.11}\right)\right]^{-2} \tag{13}$$

The absolute roughness ε that is used in Eq. 13 is a constant value that is found in table 1. The absolute roughness is a measurement of the surface roughness of a material. The roughness of a pipe influences the flow rate and pressure loss of the fluid. This is caused by the friction between the fluid and the pipe surface. (Neutrium, 2012)

Table 1 Overview of absolute roughness for different materials (Thermal engineering, 2019)

Material	**Absolute roughness ε (mm)**
Copper, Lead, Aluminium	0.001-0.002
PVC and Plastic Pipes	0.0015-0.007
Stainless Steel	0.0015
Steel Commercial Pipe	0.045-0.09
Cast Iron	0.25-0.8
Concrete	0.8-3

11.3 Minor head losses

Since the pipe system of the Ocean Battery consist of more parts than straight pipes, the head losses in these parts effect the total head of the system. The head losses of these parts are categorized as minor head losses, since in general they are smaller than the losses caused by pipe friction. However, in systems with short pipes and a large pipe diameter, it is common that the minor head losses are larger than the major head losses since the friction with the pipe surface will it that case causes relatively small losses (Engineering Division Crane, 1969). Therefore, it is important to treat the minor head losses with the same precision as the major head losses.

Minor head losses are mainly caused by obstacles and irregular shapes of the pipe. These causes are divided in the following categories:

- Bends, elbows, splits and other fittings (K_{bes})
- Turbines and pumps (K_t)
- Sudden expansion or contraction (K_{ec})
- Valves (K_v)

In order to include the minor head losses in the Darcy-Weisbach equation, the K values that represent these losses need to be selected. For K_{bes} and K_v constant values are shown in table 2. K_{ec} represents the head loss due to the sudden contraction and expansion between the reservoir or the bladder and the pipe. Both these entrances and exits are used in the pump and the turbine model. In order to calculate the value for the entrance, we use the ratio $\frac{A_p}{A_b}$, in which A_p is the area of the pipe and A_b is the area of the bladder (Neutrium,2013). When using a pipe of diameter 1, A_p is $1^2\ \frac{\pi}{4} = 0.785$. The A_b is calculated based on the design of 70m x 70m, A_b is 70 (70) = 4900. When we calculate the ratio $\frac{A_p}{A_b}$, we get $\frac{0.785}{4900} = 0.00016$. Since this ratio is nearly zero, we will use the maximum K value for the entrance, which is 0.5 . At the exit of a pipe to larger reservoir the water velocity decreases in a short time towards zero. Therefore, the K value for the exit of a pipe is always 1 (Neutrium, 2013). When the we combine the K values of the entrance and the exit of the pipe, we get: $K_{ec} = 0.5 + 1 = 1.5$

K_t is a function of the velocity and design measurements and therefore the equation that is used to determine that value is discussed in the next chapter of this research.

Table 2 K-values for valves, elbows and fittings (Engineering Division Crane, 1969)

Fitting	**Type**	**K**
Valve	Fully open	0.2
	¾ open	0.9
	½ open	4.5
	¼ open	24
90° elbow	Long radius	0.36
	short radius	0.75
Branch split		1
Pipe exit		1

Combining the above mentioned K values, the following equation is formed:

$$K_L = K_{bes} + K_t + K_{ec} + K_v \tag{14}$$

12 Flowrate of turbine model

The turbine model calculates the power output of the turbine (P_t) as a function of the flowrate. Therefore it is useful to first describe the equations that are necessary to calculate the flowrate of the turbine (Q_t). Like the pump's efficiency, the efficiency of the turbine (η_t) is depended on the flow that is running through it. When the flowrate is lower than the designed capacity of the turbine, it's efficiency will decrease. The power of the turbine is given by the following formula:

$$P_t = \rho\, g\, H_t\, Q_t\, \eta_t \tag{15}$$

where:

ρ is the density of the fluid $[kg/m^3]$
g is the standard acceleration due to gravity $[m/s^2]$
H_t is the total head of the turbine $[m]$

$$\eta_t = f(Q_t) \tag{16}$$

The turbine head (H_{tl}) equals the static head minus the head loss between the bladder and the turbine outlet (H_{tl}). For the calculations of the head loss in the turbine model the same steps are followed as with the pump head loss (Eq. 5 – Eq. 14). However, in the turbine model, the friction factor of the turbine is added to the head loss calculations. This friction factor K_t has a large influence on the flow rate and is further elaborated on in the section "Head loss due to the turbine".

The flowrate (Q_t) is depended on the water level in the reservoir and can be calculated using Bernoulli's equation (Menon, 2014):

$$\frac{p_1}{\rho g} + \frac{{v_1}^2}{2g} + h_1 = \frac{p_2}{\rho g} + \frac{{v_2}^2}{2g} + h_2 + H_{tl} \tag{17}$$

where:

p_i is the pressure at point i $[Pa]$
v_i is the velocity at point i $[m/s]$
h_i is the height of point i $[m]$

The sea level surface is considered as point 1 in this equation and the turbine outlet is point 2. The height of the turbine outlet will be set as the reference point and therefore h_2 is zero. Since surface of the sea is much large then the cross sectional area of the pipe, its velocity is much smaller than the velocity in the pipe ($v_1 \ll v_2$). Therefore, the velocity at the sea's surface is considered to be zero. At point 1 the pressure is atmospheric and at point 2 the pressure is the result of the height of the water level in the reservoir (H_r). In this equation, the depth of the system is h.

$$h = \frac{{v_2}^2}{2g} + H_{tl} + H_r \tag{18}$$

The depth (h) and the water level in the reservoir (H_r) can be combined in the static head (H_s). Since total head loss (H_{tl}) can be replaced by equation 7, the following equation can be derived from equation 18 (Menon, 2014):

$$H_s = \frac{v^2}{2g} + K\frac{v^2}{2g} \tag{19}$$

where:
K is the loss coefficient [−]

Equation 19 is rewritten in such a way that it expresses the velocity in the turbine model as a function of the static head and the total head loss in the pipes of the turbine.

$$v_t = \sqrt{\frac{2\ g\ H_s}{1+K}} \tag{20}$$

In order to get the flowrate of the turbine, the velocity is multiplied with the cross sectional area of the pipe (A). This results in the following equation for the flowrate:

$$Q_t = A * v_t = 0.25\pi {D_t}^2 \sqrt{\frac{2\ g\ H_s}{1+K}} \tag{21}$$

12.1 Head loss due to the turbine

In order to find the head loss due to the turbine, a method from earlier research (Dijkstra, 2016) is used. The general hydropower equation is the starting point of this method, and is given in equation 22 (Bansal, 2004):

$$Power = \rho\ g\ h\ Q_t\ \eta_t \tag{22}$$

A power equation is made for a point just before the turbine and one directly after the turbine:

$$Power_{in}\ \eta_t = Power_{turbine} \tag{23}$$

When the formulas for $Power_{in}$ and $Power_{turbine}$ are placed in Eq. 23, that reads as:

$$\left(\rho\ g\ h - K_f\ \frac{\rho}{2}\ v^2\right)\ Q_{in}\ \eta_t = \left(K_t\ \frac{\rho}{2}\ v^2\right) Q_{turbine} \tag{24}$$

where:
K_f is loss coefficient due to friction [−]
K_t is loss coefficient due to the turbine [−]

Since the flowrate before and in the turbine are the same, $Q_{in} = Q_{turbine}$. We can cancel out Q_{in} and $Q_{turbine}$, and then get:

$$\left(\rho\ g\ h - K_f\ \frac{\rho}{2}\ v^2\right)\ \eta_t = \left(K_t\ \frac{\rho}{2}\ v^2\right) \tag{25}$$

The left-hand side of this equation shows the pressure due to head difference that is adjusted for the friction factors in the pipe. The right-hand side show the pressure loss that occurs by the conversion from mechanical to electrical energy. Equation 25 can be rewritten for the K_t, so that head loss due to the turbine is expressed in a K value and is useable in the Darcy-Weisbach equation:

$$K_t = \frac{2\ g\ H\ \eta_t}{v^2} \tag{26}$$

12.2 Power output of the generator

In order to calculate the power output of the generator the power of the turbine (P_t) is multiplied with the efficiency of the energy conversion (η_g) from mechanical to electric energy that occurs in the generator:

$$P_g = P_t\ \eta_g \tag{27}$$

13 Simulation of the Ocean Battery

In this chapter, the methodology of the Matlab models is discussed. The methodologies are describing the steps that are followed in the simulation. The equations that are explained in the previous chapter are used to calculate the flowrates and the power input and output of the system. The Matlab codes that are created based on the methodologies of both models are included in appendices A and B of this research.

13.1 Methodology of the pump model

A) *Initialize* H_{pl} *&* H_s
B) *Find efficiency of the motor as function of* P_m*, then calculate* P_p *and send it to the pump.*
C) *While reservoir is not empty:*
    1. *Calculate* Q_p
    2. *Find efficiency of the pump as function of* Q_p
    3. *Calculate* v
    4. *Calculate Reynolds number*
    5. *Calculate* f
    6. *Calculate* K_{pipe}
    7. *Add* $K_{fittings}$ *to get* K_{total}
    8. *Calculate* H_{pl} *based on* K_{total}
    9. *Subtract* Q_p *from the volume of the reservoir*
    10. *Determine the water height in the reservoir based on the volume in the reservoir and subtract it from the depth to determine* H_s
    11. *Combine* H_s *and* H_{pl} *to get* H_p *for the next iteration.*
D) *Multiply the* P_m *with the time it took to pump all water from the reservoir to the bladder to get the total energy in.*

13.2 Methodology of the turbine model

A) *Initialize K &* H_s
B) *While reservoir is not full:*
    1. *Calculate* Q_t
    2. *Find the efficiency of the turbine as a function of the* Q_t

3. *Calculate* v
4. *Calculate Reynolds number*
5. *Calculate* f
6. *Calculate* K_{pipe}
7. *Calculate* $K_{turbine}$
8. *Add* $K_{fittings}$, K_{pipe} *&* $K_{turbine}$ *to* K_{total}
9. *Add flow rate to the volume of the reservoir*
10. *Determine the water height in the reservoir based on the volume in the reservoir and subtract it from the depth to determine* H_s
11. *Calculate the power output of the turbine*
12. *Determine the power output of the generator by multiplying the power of the turbine with the efficiency of the generator*

C) *Sum the power outputs of the generator to get the total energy out*

D) *Divide the total energy output by the total energy input to get the round trip efficiency of the system.*

13.3 Functions in the simulation

In order to calculate the efficiencies of the pump and turbine and the water level in the reservoir, external function are used in the models. The Matlab codes of these functions are included in the appendices C, D and E.

13.3.1 Efficiency (Appendices C & D)

There are no equations available that can give the efficiency based on the flowrate, since these efficiency result from testing the pumps and turbines. The efficiency functions are therefore based on the efficiency curves of centrifugal pumps and turbines. Since the pump and turbines for the system have not been selected, general centrifugal efficiency curves are used. From the curves, 10 point are chosen and between these point the Matlab function "linspace" is used to create linear lines between these points. In this way, the accuracy of the efficiency increases from 10 to 100 points. The input for the efficiency function is the flowrate of the model. Based on the flowrate and the maximum flow rate of the pump, the flowrate ratio is calculated. The flowrate ratio is used to find the efficiency from the efficiency data, as is shown in figure 4. The efficiency curves that are used in these function are based on general centrifugal pumps and turbine. When the pumps and turbines for the final design are chosen the corresponding efficiency curve can replace the curves that are currently used.

13.3.2 Water level in the reservoir (Appendix E)

This function calculates the water level in the horizontal reservoir as a function of the volume fraction. The volume fraction is found by dividing the current volume by the maximum volume of the tank. The volume fraction is linked to a data set (Barderas & Rodea, 2016) that divides a horizontal tank in 100 water levels. The corresponding height fraction is taken from the data set and multiplied with the inner diameter of the reservoir. The output of the function is the water height in the reservoir in meter.

14 Validation of the simulation

In order to validate the simulation, three methods are used. The first method is through face validity (Sargent, 2013), which is the review of an individual that is knowledgeable about the system. In the case of this research one of the stakeholders, M. van Rooij Msc., was asked whether the behaviour of the model and its results are reasonable. During a discussion with van Rooij the results were assessed to be reasonable.

The second method that is used to verify the simulation through parameter variability (Sargent, 2013). This technique consists of changing parameters in the model to check the effect on the results of the model. This technique is used by testing the effect of different element values, as is done in the chapter "Case study". The outcome of these verification tests were as expected and comparable with the changes in the outcome that resulted from the element changes that were done during the Case study.

The third method to verify the simulation uses analytical calculations in order to check the behaviour of the model. Analytical calculations are done to calculate the flowrates of the pump and the turbine model in order to check if the results are accurate. For these calculations the settings from a case study at 40 meters depth are used. In the analytical calculations the same steps are followed as in the simulation. In order to verify the results of the simulation, the flowrates are calculated for the first two time steps of both models. The flowrates that resulted from the calculations are similar to the flowrates that resulted from the simulation. An overview of the analytical calculations is included in appendix E.

Since all three methods have a positive result, the model is concluded to be validated and the test result are assumed to be accurate.

15 Case study

A case study of the system at 40 meter depth is performed. In table 3 the input values for the simulation are displayed. The result of the simulation are discussed and figures are included to get a better overview of the flows in the system. It very valuable for the stakeholders from the Ocean Grazer BV to know the effect of the separate elements on the round trip efficiency. Therefore, the system is divided in elements that can be excluded from this simulation. By doing this we can determine the effect of a specific element on the round trip efficiency. With this information the Ocean Grazer BV will gather knowledge over the elements and it is shown where most improvement in the efficiency can be achieved.

Table 3: Model parameters for case study

Constant	Value
Power input	1 MW (1000000 W)
Efficiency of the motor	92%
Efficiency of the turbine	92%
Depth	40 m
Inner diameter reservoir	9 m
Length reservoir	80 m
Pipe length	20 m
Diameter pipe	1 m
Material roughness pipe (steel)	0.000045 m
K splitting	1
K valve	0.2
K elbow	0.36
K entrance	1.5

15.1 Results

When these values are used in the simulation of the pump model, the flowrate and the total energy input are calculated. The graph of the flowrate and the efficiency of the pump are shown in figure 5. The static head of the pump increases over time, since the

water level in the reservoir decreases when the water is pumped to the bladder. As a result, the pump will have to deliver more power to pump a cubic meter of water to the bladder. Since the power input stays constant, the flowrate decreases over time, as can be seen in blue graph in figure 5. When the time is 1000 seconds, there is a small bend in the graph. This bend occurs since the highest efficiency of the pump is reached at this point. And afterwards the efficiency will start to decrease again, as is shown by the orange graph in figure 5. Since the power input of the motor is constant, the energy input is calculated by multiplying the power input of the motor with the time it takes to fill the bladder. As is shown in figure 5, the bladder is filled in 2220 seconds. Since the power input is 1 MW (1000000 W), the total energy the system is: $2220 * 1 = 2220$ MJ.

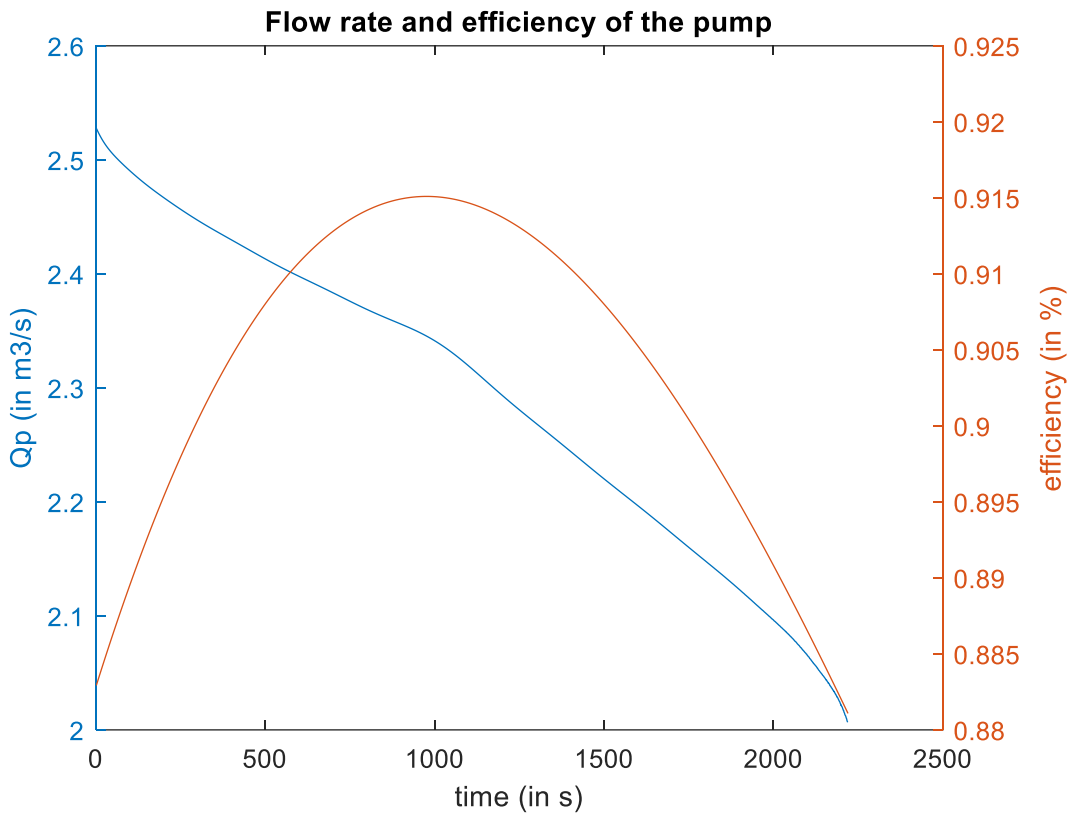

Figure 5: flowrate (Q_p in m3/s)) and efficiency (in %) of the pump model

The same values from table 3 are used in the turbine model, and the resulting flowrate of the turbine model is shown in figure 6. Again, the steps in the height of the reservoir can be recognized from the graph. Over time, the water level in the reservoir increases and therefore the static height will decrease. As a result the flowrate of the pump will also decrease, as is shown in figure 6.

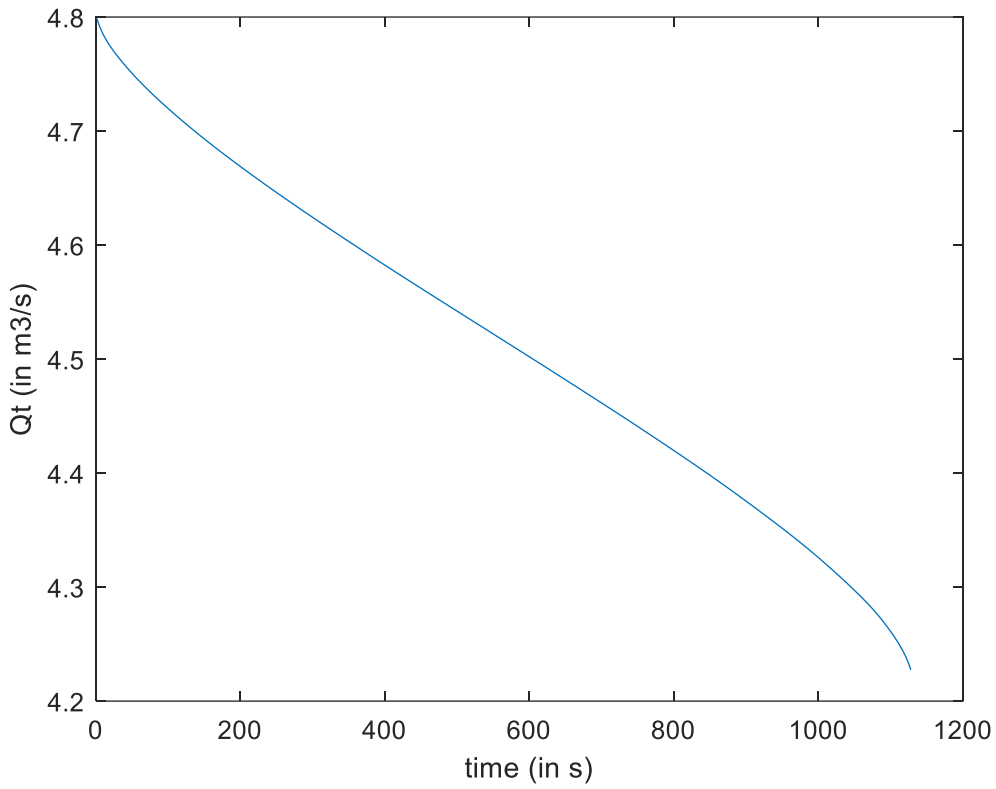

Figure 6: flowrate (Q_t in m^3/s) of the turbine model

The power output of the turbine is shown in figure 7. The graph behaviour of the power output graph is comparable to the graph of the turbine flowrate. However, the difference is that the variable turbine efficiency is integrated in the power output. The maximum efficiency of the turbine occurs at ~650 seconds, as can be seen from the orange graph in figure 7. The total energy output of the turbine is found by the sum of all power outputs of the turbine, that is equal to 1359.6MJ. This total value is multiplied with the efficiency of the generator, 92%, equal to the efficiency of the motor. The total energy output of the generator is then calculated to be 1250.8 MJ.

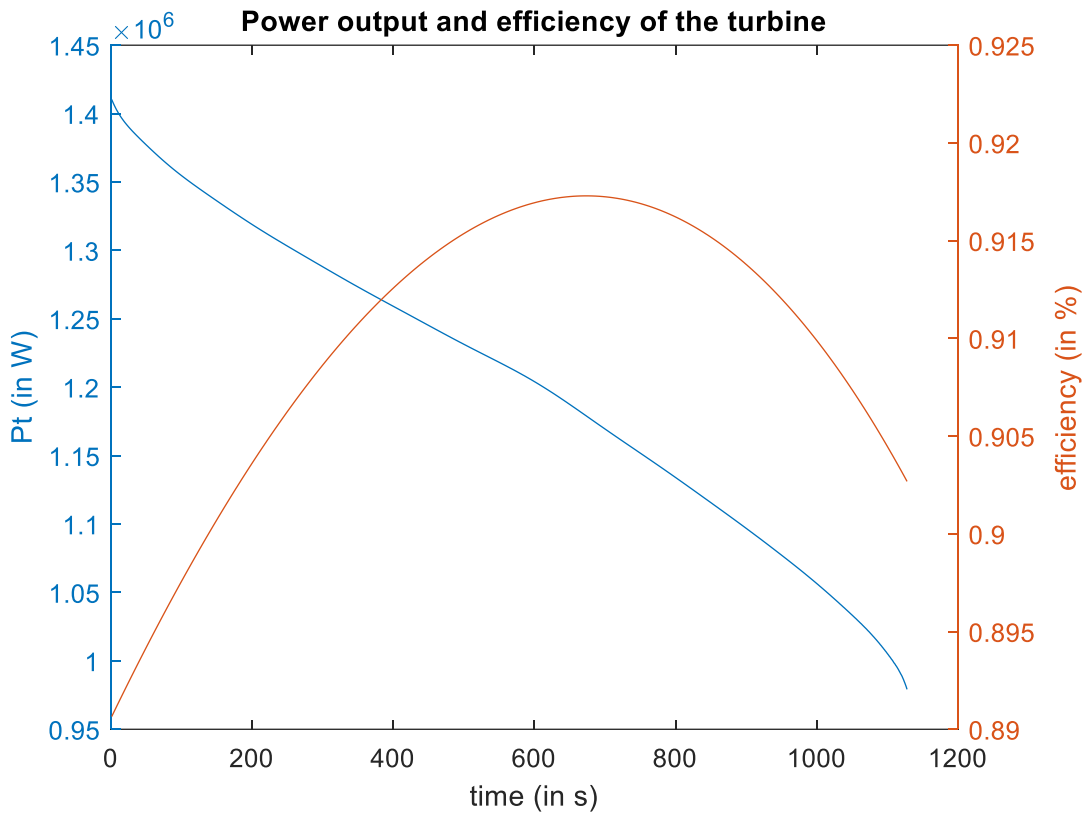

Figure 7: Power output (Pt in W) and efficiency (in %) of the turbine

The round trip efficiency of the system is determined by dividing the total energy in by the total energy out. This results in: $\frac{1250.8}{2220} * 100 = 56.34\%$. Therefore, the round trip efficiency of the Ocean Battery with the settings from table 3 is calculated to be 56.34%.

15.2 Element analysis

In order to find the effect of the separate elements on this round trip efficiency, the elements are left out in turn from the simulation. The elements that are tested are:

- Straight pipe
- Splitting in the pipe
- Bends in the pipe
- Open valve
- Contraction at the entrance of the pipe
- Material surface roughness

Table 4: Element analysis: K-value, roundtrip efficiency with/without element and effect on the roundtrip efficiency

Element	K-value	% With	% Without	% Effect on RTE
Straight pipe friction	~0.24	57.93	58.74	0.81
Splitting in the pipe	1	57.93	61.50	3.49
Bend in the pipe	0.6	57.93	60.01	2.08
Open valve	0.2	57.93	58.60	0.67
Entrance & exit of the pipe	1.5	57.93	63.49	5.56
Concrete pipe	~0.43	57.26	57.93	0.67
Very smooth steel pipe	~0.20	58.05	57.93	0.12

By analysing table 4, we can conclude that the round trip efficiency will decrease for every K-value that is added to the system. For example, adding an extra bend with K-value 0.6 will decrease the roundtrip efficiency with 2.08%. During the interview with the stakeholders it is discussed that steel pipes are preferred. Regular steel pipes are assigned a K-value of ~0.24 and will result in an roundtrip efficiency of 57.93%. In order to improve the efficiency, a smoother steel pipe can be used. This will result in an increase of 0.12% in the roundtrip efficiency. Concrete can also be chosen as an alternative material for the piping structure. However, this will result in a decrease in the roundtrip efficiency of 0.67%. When we combine the results from the element analysis, we find that adding a K value of 1 to the system will result in a efficiency decrease of 3.4%.

16 Discussion

The simulation helps in the understanding of the energy flow of the Ocean Battery. It shows the behaviour of the flowrates and the power output and calculates the round trip efficiency of the system. The model is validated with analytical calculations and is assessed as accurate. Based on the results from the case study the round trip efficiency is found and an element analysis is performed for the system at 40 meter depth. The round trip efficiency that is found is 56.34%. The results and the element analysis are further discussed in this section.

The use of dynamical values in the simulation increases the precision of the calculations for the round trip efficiency. In earlier research about the Ocean Grazer the values for pipe friction, turbine friction and pump and turbine efficiency were considered as fixed values. However, these values depend on pipe diameter, pipe material and water velocity.

The friction between the pipe surface and the fluid is a small factor in the energy loss of the system. The energy losses due to friction (major losses) were expected to be higher than the energy losses due to bends and fittings (minor losses) since that is the way they relate in most systems. However, due to the relatively short and wide pipes that are used in the Ocean Battery, it can be explained why the major losses are smaller than the minor losses.

The splitting and bends have large K values and therefore result in large energy losses. Therefore, the use of T-branches and bends should be kept to a minimum when designing the piping system to maximize the round trip efficiency. The K values of the bends and fittings can be used to determine their effect on the efficiency. From the case

study it can be determined that adding an element with K value 1 will decrease the efficiency with ~3.4%

The efficiency of the motor, pump, turbine and generator have a large impact on the energy losses in the system. Therefore their capacity should be selected with high precision based on the expected and designed flowrates.

Other pumped hydro storage systems report to have efficiencies of 65%-75% (Rehman et al., 2015). When we compare the round trip efficiency of the Ocean Battery that is found in this research with the efficiencies from Rehman, we can conclude that this is lower than the alternatives. An important factor to take in consideration in the comparison is that in regular pumped hydro storage use mountain basins, in which the water level will not vary as much as it does in this system. In the Ocean Battery, the static height varies between 31 and 40 meter, which is a 22.5% difference. The amount of water pumped with the highest efficiency of the pump is therefore smaller then with regular pumped hydro systems in which static height will vary less. Every pump type has its own efficiency curve, the pump chosen for the case study might not be optimal as it was chosen based on the current design. Therefore, it would be valuable to do further research in the optimal pump type for the Ocean Battery.

Another influence that results in a lower round trip efficiency is the use of bends and branches. In regular pumped hydro storage systems, the pipes are relatively straight and do not contain branches. In the design of the Ocean Battery, a branch is used to divide the water between the inner and the outer reservoir. It is analysed in the element analysis of this research, that the branch and the bend in the current design result in an efficiency loss of 5.57%. Therefore, it would be valuable to do further research in the optimization of the design and the structure of the pipes between the reservoir and the bladder.

16.1 Limitations

In this research the influence of the depth on the energy flow and the round trip efficiency is not covered. Another case study could be performed to find the round trip efficiency at 100 meter depth. The results of that case study could be compared to the results from the 40 meter depth case study. Comparing these result can give more insight in the influence of the depth of the system.

The K values from this research are gathered from literature and are representing the elements that are in the current design of the Ocean Battery. However, the best way to calculate the K values from elements is by collecting them from test that are performed on the elements that are used in the system. By collecting the K values from tests the simulation's results would be even more accurate.

17 Conclusion

The goal of this research is to deliver insight in the round trip energy efficiency of the Ocean Battery under changeable circumstances and settings. In order to complete this goal first the information is gathered about the energy flow in the system. Theory about the conversion from electric to mechanic energy is collected and the equations that are needed to determine the flowrates of the system are described. Second, the development of the model is described in steps that need to be followed by the simulation. Third, the system is simulated in a case study. The settings that are used in the case study are based on the real world system of the Ocean Battery. Based on the results from the case study the round trip efficiency is found and an element analysis is performed. The round trip efficiency that is found is 56.34%. This efficiency can be

influenced by changing the different elements that are used in the system. In the element analysis it is found that the bend, valve and splitting in the piping structure result in large energy losses. In this research the friction of these elements is described by a K value. When a K value of 1 is added to the system, this will decrease the round trip efficiency with ~3.4%. This information about the elements useful when redesigning the piping structure in the Ocean Battery. The energy that is lost due to pipe friction is smaller than expected but can be influenced by the choice of pipe material to minimize the energy losses. The efficiency of the energy conversions in the motor, pump, turbine and generator are very important factors in the energy flow. These should be selected based on the right flow rate of the system.

18 Bibliography

Arifujjaman, M. 2015, A comprehensive power loss, efficiency, reliability and cost calculation of a 1 MW/500 kWh battery based energy storage system for frequency regulation application.

Awan, A.B., Zubair, M., Sidhu, G.A.S., Bhatti, A.R. & Abo-Khalil, A. 2019, "Performance analysis of various hybrid renewable energy systems using battery, hydrogen, and pumped hydro-based storage units", *International Journal of Energy Research,* vol. 43, no. 12, pp. 6296-6321.

Bansal, R. 2004, *A textbook of fluid mechanics and hydraulic machines,* Laxmi Publications.

Barderas, A.V. & Rodea, B.S.G. 2016, "How To Calculate the Volumes of Partially Full Tanks", Proceedings of the International Journal of Research in Engineering and Technology, , pp. 2-7.

Chen, N.H. 1979, "An explicit equation for friction factor in pipe", *Industrial & Engineering Chemistry Fundamentals,* vol. 18, no. 3, pp. 296-297.

Connor. N. 2019, Thermal engineering, Major Head Loss, viewed on 10 January 2020, <https://www.thermal-engineering.org/what-is-major-head-loss-friction-loss-definition/>

Dijkstra H.T, J.J. Barradas-Berglind, H. Meijer, M. van Rooij, W.A. Prins, A. I. Vakis & B. Jayawardhana 2016. Revenue Optimization for the Ocean Grazer Wave Energy Converter through Storage Utilization.

Engineering Division Crane. 1969, Flow of fluids through valves, fittings, and pipe, Engineering Division Crane, New York.

Hahn, H., Hau, D., Dick, C. & Puchta, M. 2017, Techno-economic assessment of a subsea energy storage technology for power balancing services.

Korpaas, M., Holen, A.T. & Hildrum, R. 2003, Operation and sizing of energy storage for wind power plants in a market system.

Lee B, Gushee D. Massive electricity storage, An AIChE paper; June 2008

Menon, E. S. (2014) Piping calculations manual. New York: McGraw-Hill (McGraw-Hill calculations).

Morgan, R., Nelmes, S., Gibson, E. & Brett, G. 2015, Liquid air energy storage – Analysis and first results from a pilot scale demonstration plant

Mousavi, N., Kothapalli, G., Habibi, D., Khiadani, M. & Das, C.K. 2019, "An improved mathematical model for a pumped hydro storage system considering electrical, mechanical, and hydraulic losses", *Applied Energy,* vol. 247, pp. 228-236.

Neutrium 2012, Absolute roughness of pipe material, viewed 1 December 2019, <https://neutrium.net/fluid_flow/absolute-roughness/>

Neutrium 2013, Pressure loss from pipe entrances and exits, viewed 7 December 2019, <https://neutrium.net/fluid_flow/pressure-loss-from-pipe-entrances-and-exits/>

Offshore hybrid renewable energy harvest and storage device [Online]. Available: <https://oceangrazer.com>

Rehman, S., Al-Hadhrami, L. M. and Alam, M. M. (2015) “Pumped Hydro Energy Storage System: A Technological Review,” Renewable and Sustainable Energy Reviews, 44, pp. 586–598.

Sardianou E. & Genoudi, P. 2013, "Which factors affect the willingness of consumers to adopt renewable energies?", Renewable Energy, vol. 57, pp. 1-4.

Sargent, R. G.. Verification and validation of simulation models. Journal of Sim 2013; 7: 12-14

Tidal barrage 2015, Isle of Withorn, viewed on 13 January 2020, http://www.esru.strath.ac.uk/EandE/Web_sites/14-15/Tidal_barrage/turbine.html>

Yang, Chi-Jen. Pumped hydroelectric storage Duke University; 2012

19 Appendix A: Pump model

```
Lp = 20; % length of the pipe in pumping stage
Ltresv = 80; % total length of the reservoir in m
Dinresv = 9; % inner diameter of the reservoir in m
Depth = 40; %Depth of the system, is used to find Hs for every Vresv
Dp = 1; % diameter of the pipe during pumping stage

% Constant parameters
miu =0.001; % viscosity of water
Rho = 1000; % density of water
g = 9.81; % gravitational constant
elbows = 1; % number of elbows in the pipes
Ktsplit = 1; % value for a branch
Kvalve = 0.2; % value for a valve
Kelbow = 0.36; % value for an elbow
Kcontr= 1.5; % value for the contraction
e = 0.000045;  % material roughness of steel pipe
Vresvmax = pi*(Dinresv/2)^2*Ltresv; % Maximum volume of the reservoir

Pm = 1000000; % power input to the motor in W

Np(1)=0.8840; % initialize efficiency
Vresv_0=0; % initialize Vresv
Vresv(1)=Vresv_0;
Hpl_0 = 1.8; % initialize Hpl
Hp(1) = Depth-Dinresv+Hpl_0;
Nm = N_m(Pm);   % Motor efficiency (Nm) is a function of input Pm
Pp = Pm*Nm;   % Power of the pump is a function of the Power input and the
motor efficiency
Kfittings = Kelbow*elbows+Ktsplit+Kvalve+Kcontr;     % Kfittings, the minor
losses (losses in splittings, elbows and valves)

i=1;
while Vresv<Vresvmax
    Qp(i) = (Pp*Np(i))/(Rho*g*Hp(i));
      % Flowrate in pump model
    Np(i+1) =N_P(Qp(i));
      % Efficiency of the pump is a function of the flow rate
    v(i) = Qp(i)/(0.25*pi*Dp^2);
      % Velocity
    Re(i) = (Rho*v(i)*Dp)/miu;
      % Reynolds number, function of velocity
    f(i) = (1.8*log((6.9/Re(i))+((e/Dp)/3.7)^1.11)^-2);
      % friction factor f
    Kpipe(i) = (f(i)*Lp)/Dp;
      % Major frictional losses (losses in pipes)
    K(i) = Kpipe(i) + Kfittings;
      % Total friction coefficient K
    Hpl(i) = (K(i) * v(i)^2)/ (2 * g);
      % Total head loss between reservoir and bladder
    Vresv(i+1) = Vresv(i) + Qp(i);
      % Amount of water in the reservoir (m^3)
    Hs(i) = Heightresv(Vresv(i+1), 9, Vresvmax)+ Depth - Dinresv;
      % Water height in the reservoir
    Hp(i+1) = Hs(i)+Hpl(i);
      % Total head of the system
    i=i+1;

end
```

```
Ein= (i *Pm)/10^6
      % Total energy input in Mega joule
plot(Qp)
      % Show plot of the pumping flowrate
```

20 Appendix B: Turbine model

```
Lt = 20;  % length of the pipe in turbine stage
Ltresv = 80; % total length of the reservoir in m
Dinresv = 9; % inner diameter of the reservoir in m
Depth = 40; %Depth of the system, is used to find Hs for every Vresv
Dt = 1; % diameter of the pipe during turbine stage

% Constant parameters
miu =0.001; % viscosity of water
Rho = 1000; % density of water
g = 9.81; % gravitational constant

Ng=0.92;    % efficiency of the generator
elbows = 1; % number of elbows in the pipes
Ktsplit = 1; % value for a tee split, branched flow
Kvalve = 0.2; % value for a valve
Kelbow =0.36; % value for pipe elbow
Kcontr= 1.5; % value for the contraction
e =0.000045;  % material roughness of steel pipe
Vresvmax = pi*(Dinresv/2)^2*Ltresv; % Maximum volume of the reservoir

Htl_0 = 0; % initialize Htl
Nt(1)=0.9; % initialize Nt
Vresv(1)= Vresvmax; % initialize Vresv to Vresvmax. At the start of turbine
phase the bladder is full.
Hs(1)=Depth; % initialize static head to Depth of the system
Kfittings = Kelbow*elbows+Ktsplit+Kvalve+Kcontr;   % Kfittings, the minor
losses (losses in splittings,elbows and valves)
K(1)=20; initialize K
i=1;

while Vresv(i)>0

    Qt(i) = (0.25*pi*Dt^2)*sqrt(2*g*Hs(i)/(1+K(i)));
      % Flowrate in turbine model
    Nt(i) = N_T(Qt(i));
      % Efficiency of the turbine is a function of the flow rate
    v(i) = Qt(i)/(0.25*pi*Dt^2);
      % Velocity
    Re(i) = ((Rho*v(i)*Dt)/miu);
      % Reynolds number, function of velocity
    f(i) = (1.8*log((6.9/Re(i))+((e/Dt)/3.7)^1.11)^-2);
      % friction factor f
    Kpipe(i) = (f(i)*Lt)/Dt;
      % Major frictional losses (losses in pipes)
    Kturbine(i) =(2*g*(Depth-(Dinresv/2))*0.9/(6.125^2));
    K(i+1) =Kpipe(i)+Kturbine(i)+Kfittings;
      % Total friction coefficient K
    Vresv(i+1) = Vresv(i) - Qt(i);
```

```
      % Amount of water in the reservoir (m^3)
    Hs(i+1) = Depth-Dinresv+Heightresv(Vresv(i+1), 9, Vresvmax);
      % Waterheight in the reservoir
    Htl(i)=Hs(i+1)-(((Kpipe(i)+Kfittings)*v(i)^2)/(2*g));
      % Total head loss between reservoir and bladder
    Pt(i) = Qt(i)*Htl(i)*Rho*g*Nt(i);
      % Power output of the turbine
    Pg(i) = Pt(i)*Ng;
      % power output generator
    i=i+1;
end
plot(Qt)

Results = [Qt Pt/1000000];
Eout = sum(Pt)/10^6
Eout = sum(Pg)/10^6  % Total energy output in Mega Joule
efficiency=Eout/Ein  % Roundtrip efficiency of the Ocean Battery
```

21 Appendix C: Efficiency functions

21.1 Efficiency of the pump

```
function [Np] = N_P(Qp)
% this function shows the  pump efficiency as a function of the flowrate Qp
used in the Ocean Battery
N = 100;        % accuracy
Qmax = 2.6;     % maximum flowrate of the pump
Qratio =Qp/Qmax;
Qratio = round(Qratio*10*N);

 E = [];
 D = [0 0 0 0.39 0.59 0.69 0.79 0.85 0.89 0.92 0.87];
 G1 = linspace(D(1),D(2),N+1);
 G = G1;
 for i=2:10
    Gi = linspace(D(i),D(i+1),N+1);
    G = [G Gi(2:N+1)];
 end
 Np = G(Qratio+1);
end
```

21.2 Efficiency of the Turbine

```
function [Nt] = N_T(Qt)
% this function shows the turbine efficiency as a function of the flowrate
Qt used in the Ocean Battery
N = 100; % accuracy
Qmax = 5;  % maximum flowrate of the pump
Qratio = Qt/Qmax;
Qratio = round(Qratio*10*N);

 E = [];

 D = [0 0 0 0.39 0.59 0.69 0.79 0.85 0.89 0.92 0.87];
 G1 = linspace(D(1),D(2),N+1);
 G = G1;
 for i=2:10
    Gi = linspace(D(i),D(i+1),N+1);
    G = [G Gi(2:N+1)];
 end
```

```
 Nt = G(Qratio+1);
end
```

22 Appendix D: Water height in the reservoir

```
function [Hresv] = Heightresv(Vresv, Dinresv, Vresvmax)
% this function shows the  water height in the reservoir as a function of
the amount of water that is in the reservoir (Vresv)

volumefraction=Vresv/Vresvmax;

C= [ 0 0.00169  0.00477 0.00874 0.01342 0.01869 0.02450 0.03077 0.03748
0.04458 0.05204 0.05985 0.06797 0.07639 0.08509 0.09406 0.10327 0.11273
0.12240 0.13229 0.14238 0.15266 0.16312 0.17375 0.18455 0.19550 0.20660
0.21784 0.22921 0.24070 0.25231 0.26348 0.27587 0.28779 0.29981 0.31192
0.32410 0.33636 0.34869 0.36108 0.37353 0.38603 0.39858 0.41116 0.42379
0.43644 0.44912 0.46182 0.47454 0.48727 0.50000 0.51273 0.52546 0.53818
0.55088 0.56356 0.57621 0.58884 0.60142 0.61397 0.62647 0.63892 0.65131
0.66364 0.67590 0.68808 0.70019 0.71221 0.72413 0.73652 0.74769 0.75930
0.77079 0.78216 0.79340 0.80450 0.81545 0.82625 0.83688 0.84734 0.85762
0.86771 0.87760 0.88727 0.89673 0.90594 0.91491 0.92361 0.93203 0.94015
0.94796 0.95542 0.96252 0.96923 0.97550 0.98131 0.98658 0.99126 0.99523
0.99831 1.000];

X=Dinresv;
for o=1:101;
 Verror(o) = abs(volumefraction-C(o));
end
 G = [];
 E = 0:0.01:1
 D = min(Verror);
 K=find(Verror==D);
 G = [Verror;E];
 HD = G(2,K);
 Hresv=HD*X;
```

23 Appendix E: Analytical calculations

23.1 Validation of the pump model

$$P_p = P_m * \eta_m \;\; = \;\; 1000000 * 0.92 = 920000\ W$$

$$Q_p = \frac{P_p * \eta_p}{\rho * g * H_p} = \frac{920000 * 1}{1000 * 9.81 * 36} = 2.605\ \frac{m^3}{s}$$

$$\eta_p\,(Qp) = \eta_p\,(2.605) = 0.89$$

$$v = \frac{Qp}{0.25 * \pi * {D_p}^2} = \frac{2.605}{0.25 * \pi * 1^2} = 3.317\ \frac{m}{s}$$

$$Re = \frac{\rho * v * D_p}{\mu} = \frac{1000 * 3.317 * 1}{0.001} = 3316854.6$$

$$f = \left[1.8 * \log\left(\frac{6.9}{Re}\right) + \left(\frac{\frac{\varepsilon}{D_p}}{3.7}\right)^{1.11}\right]^{-2} = \left[1.8 * \log\left(\frac{6.9}{3316854.6}\right) + \left(\frac{\frac{0.000045}{1}}{3.7}\right)^{1.11}\right]^{-2} = 0.0118$$

$$K_{pipe} = \frac{f * L_p}{D_t} = \frac{0.01184 * 20}{1} = 0.223$$

$$K_{pl} = K_{pipe} + K_{ec} + K_{bes} + K_v = 0.223 + 0.2 + 0.36 + 1.5 + 1 = 3.283$$

$$H_{pl} = \frac{K * v^2}{2 * g} = \frac{3.283 * 3.317^2}{2 * 9.81} = 1.84\ m$$

$$Vresv = Vresv - Qp = 5089.4 - 2.605 = 5086.795\ m^3$$

$$H_s = Depth - Dinresv = 40 - 9 = 31\ m$$

$$H_p = H_s + H_{pl} = 31 + 1.84 = 32.84\ m$$

$$Q_p = \frac{P_p * \eta_p}{\rho * g * H_p} = \frac{920000 * 0.89}{1000 * 9.81 * 32.84} = 2.542\ \frac{m^3}{s}$$

23.2 Validation of the turbine model

$$Q_t = 0.25 * \pi * {D_t}^2 \sqrt{\frac{2 * g * H_s}{1 + K}} = 0.25 * \pi * 1^2 \sqrt{\frac{2 * 9.81 * 40}{1 + 20}} = 4.801\ \frac{m^3}{s}$$

$$\eta_t\,(Q_t) = \eta_t(4.801) = 0.89$$

$$v = \frac{Q_t}{0.25 * \pi * {D_t}^2} = \frac{4.801}{0.25 * \pi * 1^2} = 6.113\ \frac{m}{s}$$

$$Re = \frac{\rho * v * D_t}{\mu} = \frac{1000 * 6.113 * 1}{0.001} = 6113217.53$$

$$f = \left[1.8 * \log\left(\frac{6.9}{Re}\right) + \left(\frac{\frac{\varepsilon}{D_p}}{3.7}\right)^{1.11}\right]^{-2} = \left[1.8 * \log\left(\frac{6.9}{6113217.53}\right) + \left(\frac{\frac{0.000045}{1}}{3.7}\right)^{1.11}\right]^{-2} = 0.01085$$

$$K_{pipe} = \frac{f * L_t}{D_t} = \frac{0.01085 * 20}{1} = 0.2169$$

$$K_{turbine} = \frac{2 * g * H_s * \eta_m}{v^2} = \frac{2 * 9.81 * 35.5 * 0.9}{6.1132} = 16.709$$

$$K_{pl} = K_{turbine} + K_{pipe} + K_{ec} + K_{bes} + K_v = 16.709 + 0.2169 + 0.36 + 1.5 + 1 + 1.36 = 19.986$$

$$H_s = Depth - H_{resv} = 40 - 0 = 40\,m$$

$$H_{tl} = H_s - \frac{(K_{pipe} + K_{ec} + K_{bes} + K_v) * v^2}{2 * g} = 40 - \frac{3.2769 * 6.11^2}{2 * 9.81} = 33.758\,m$$

$$Vresv = Vresv - Qp = 5089.4 - 4.8013 = 5084.6\,m^3$$

$$P_t = Q_p * \ H_{tl} * \rho * g * \eta_t \ = \ 4.8013 * 33.758 * 1000 * 9.81 * 0.89 = 1415124.22\ \mathrm{W}$$

$$Q_t = 0.25 * \pi * {D_t}^2 \sqrt{\frac{2 * g * H_s}{1 + K}} = 0.25 * \pi * 1^2 \sqrt{\frac{2 * 9.81 * 40}{1 + 19.986}} = 4.803\ \frac{m^3}{s}$$